AFRL-RX-WP-JA-2019-0147

CHARACTERIZATION OF MICROTEXTURE REGIONS IN Ti ALLOYS USING EDDY CURRENT TESTING (PREPRINT)

Matthew R. Cherry, Daniel Sparkman, and Adam Pilchak

AFRL/RX

Laura Homa

University of Dayton Research Institute

30 NOVEMBER 2018
Interim Report

(STINFO COPY)

AIR FORCE RESEARCH LABORATORY
MATERIALS AND MANUFACTURING DIRECTORATE
WRIGHT-PATTERSON AIR FORCE BASE, OH 45433-7750
AIR FORCE MATERIEL COMMAND
UNITED STATES AIR FORCE

REPORT DOCUMENTATION PAGE

Form Approved
OMB No. 0704-0188

1. REPORT DATE *(DD-MM-YY)*	2. REPORT TYPE	3. DATES COVERED *(From - To)*
30 November 2018	Interim	3 March 2014 – 30 October 2018

4. TITLE AND SUBTITLE
CHARACTERIZATION OF MICROTEXTURE REGIONS IN TI ALLOYS USING EDDY CURRENT TESTING (PREPRINT)

5a. CONTRACT NUMBER
IN-HOUSE

5b. GRANT NUMBER

5c. PROGRAM ELEMENT NUMBER

6. AUTHOR(S)
1) Matthew R. Cherry, Daniel Sparkman, and Adam Pilchak - AFRL/RX
2) Laura Homa – UDRI

5d. PROJECT NUMBER

5e. TASK NUMBER

5f. WORK UNIT NUMBER
X0UK

7. PERFORMING ORGANIZATION NAME(S) AND ADDRESS(ES)
1) AFRL/RX
Wright-Patterson AFB
Dayton, OH 45433
2) University of Dayton Research Institute
300 College Park Ave.
Dayton, OH 45469

8. PERFORMING ORGANIZATION REPORT NUMBER

9. SPONSORING/MONITORING AGENCY NAME(S) AND ADDRESS(ES)
Air Force Research Laboratory
Materials and Manufacturing Directorate
Wright-Patterson Air Force Base, OH 45433-7750
Air Force Materiel Command
United States Air Force

10. SPONSORING/MONITORING AGENCY ACRONYM(S)
AFRL/RXCA

11. SPONSORING/MONITORING AGENCY REPORT NUMBER(S)
AFRL-RX-WP-JA-2019-0147

12. DISTRIBUTION/AVAILABILITY STATEMENT
DISTRIBUTION STATEMENT A. Approved for public release: distribution is unlimited.

13. SUPPLEMENTARY NOTES
PA Case Number: 88ABW-2018-6017; Clearance Date: 30 Nov 2018. This document contains color. Journal article published in AIP Conference Proceedings, Vol. 2102, No. 1, 8 May 2019.
The final publication is available at https://doi.org/10.1063/1.5099816

14. ABSTRACT *(Maximum 200 words)*
Quantitative characterization of impact damage in polymer matrix composites (PMCs) with ultrasonic inspection is desired to enable improved prediction of damage evolution for lifing of composite structures. Post-processing of single-sided pulse-echo Ultrasonic Test Microtexture region (MTR) formation in engine components made from titanium alloys has been shown to significantly reduce the dwell fatigue life of the components. Specifically, when the MTR is large enough and the c-axis is oriented in a specific direction relative to the loading axis, cracks in MTRs can grow much more rapidly than predicted by traditional fracture mechanics. It has been shown that eddy current methods are sensitive to MTR formation on a bulk scale, but no study has been done to assess the fundamental limitations of eddy current methods for detecting specific MTRs. In this work, the sensitivity of eddy current sensors to MTRs at specific orientations with respect to the surface area and the volumetric depths was analyzed in a modeling and simulation framework. One MTR in a host of otherwise randomly oriented single crystals was simulated, varying the size and orientation parameters. The eddy current signals were predicted using a previously developed approximation based model

15. SUBJECT TERMS
Microtexture region (MTR); titanium (Ti) alloys; eddy current testing; polymer matrix composites (PMCs); engine; fracture

16. SECURITY CLASSIFICATION OF:			17. LIMITATION OF ABSTRACT:	18. NUMBER OF PAGES	19a. NAME OF RESPONSIBLE PERSON (Monitor)
a. REPORT	b. ABSTRACT	c. THIS PAGE			Michael Uchic
Unclassified	Unclassified	Unclassified	SAR	9	19b. TELEPHONE NUMBER *(Include Area Code)* (937) 255-0594

Characterization of Microtexture Regions in Ti Alloys Using Eddy Current Testing

Matthew R. Cherry[1, a)], Daniel Sparkman[1], Adam Pilchak[1], and Laura Homa[1,2]

[1]*Air Force Research Laboratory, Materials and Manufacturing Directorate, Wright-Patterson AFB, OH, USA.*
[2]*University of Dayton Research Institute, Structural Integrity Division, Dayton, OH, USA.*

[a)]Corresponding author: matthew.cherry.2@us.af.mil

Abstract. Microtexture region (MTR) formation in engine components made from titanium alloys has been shown to significantly reduce the dwell fatigue life of the components. Specifically, when the MTR is large enough and the c-axis is oriented in a specific direction relative to the loading axis, cracks in MTRs can grow much more rapidly than predicted by traditional fracture mechanics. It has been shown that eddy current methods are sensitive to MTR formation on a bulk scale, but no study has been done to assess the fundamental limitations of eddy current methods for detecting specific MTRs. In this work, the sensitivity of eddy current sensors to MTRs at specific orientations with respect to the surface area and the volumetric depths was analyzed in a modeling and simulation framework. One MTR in a host of otherwise randomly oriented single crystals was simulated, varying the size and orientation parameters. The eddy current signals were predicted using a previously developed approximation based model. Both reflection differential as well as absolute coils were analyzed in this work.

INTRODUCTION

MTR formation can have a dramatic effect on the life of a component [1]. Understanding the life of individual components made from materials that contain significant MTRs requires a method to find and characterize MTRs. To date, the primary method for accomplishing this has been using microscopy methods such as Electron Backscatter Diffraction (EBSD). Unfortunately, this method has severe limitations on the area/volume that can be interrogated. Polarized light microscopy can also be used for quantitative characterization of a surface of materials that are anisotropic in their optical properties. However, this technique cannot be used on as-machined surfaces. Lastly, surface wave microscopy techniques such as acoustic microscopy (AM) [2] or spatially resolved acoustic spectroscopy (SRAS) [3] can be used to determine the orientation/elastic properties locally over a large area of a sample. These techniques may be more robust to surface finish than other microscopy techniques, but they require added instrumentation not available in the current in-service environment. Traditional nondestructive evaluation (NDE) techniques such as eddy current (ECT) and bulk wave ultrasound (UT) have been shown to be sensitive to large areas filled with MTRs and have even been shown to be capable of detecting specific MTRs in certain materials. The spatial resolution of these techniques is larger relative to the microscopy techniques mentioned here [4]. However, these techniques are more robust to surface finish; they are routinely applied for flaw detection for in-service components. Furthermore, the infrastructure for their implementation is already in place in the service environment. This greatly incentivizes an NDE solution for MTR detection.

There are multiple challenges that currently inhibit the application of NDE techniques for MTR detection. MTRs typically do not exist in an otherwise heterogeneous host. In fact, MTRs typically form in regions surrounded by other MTRs. Thus, when trying to characterize a specific MTR, the signals from surrounding MTRs confound the detection capability. As an added challenge, only MTRs of a specific size, orientation and location are of interest. This implies that an NDE technique must be selective in the detection of MTRs to avoid false calls. The NDE method should be either a) sensitive only to specific orientations or b) capable of characterizing the orientation so that only the MTRs of interest are found. To date, traditional NDE techniques have never been shown to be capable of detecting MTRs with the required selectivity. In this work, eddy current is explored as a means to detect and characterize specific MTRs. An eddy current solution is highly desired for this problem as engine components are already largely inspected using eddy current. Furthermore, there has been work that has shown that eddy current is sensitive to surface breaking MTRs. However, no systematic study showing the detection limits and the discriminatory capability of eddy current for detection of MTRs has been done.

45th Annual Review of Progress in Quantitative Nondestructive Evaluation, Volume 38
AIP Conf. Proc. 2102, 080008-1–080008-7; https://doi.org/10.1063/1.5099816
Published by AIP Publishing. 978-0-7354-1832-5/$30.00

One significant issue for understanding the limits of detectability of MTRs using NDE techniques is that there are no reference standards or probability of detection sample sets that can be used to assess the NDE technique. Large volumes of materials have been analyzed previously using EBSD to determine the location and sizes of MTRs in samples. However, NDE techniques are often volumetric and require knowledge of the subsurface behavior of the MTR to fully understand signals from the samples. Furthermore, no information is typically available in these samples about subsurface MTRs. Thus, in this work, a pipeline for predicting the eddy current signal over samples that are generated digitally was established. Synthetic sample builders were used to generate digital samples with large regions of texture in them. An eddy current model developed in previous efforts was used to predict the signals from eddy current probes in these samples. These results were used to show signal changes from one region to another as a function of misorientation of the c-axis between two large textured regions. These signatures were shown to have a distinct behavior in the c-axis relative to the response from cracks and notches. This paper describes the progress to date on model development and validation.

EDDY CURRENT MODEL

The eddy current model used in this work was previously discussed in [5]. This model uses the Born approximation to reduce the governing equations for eddy current to numerical integrals. In this way, there is no matrix inversion such as that required by traditional numerical methods for solving eddy current problems. A brief introduction to this model is given here.

Absolute Coil Model

The impedance change of an eddy current coil due to a change in conductivity of some region within a conductor can be expressed as [6]:

$$\Delta Z = \frac{1}{I^2}\int_V [i\omega \mathbf{H}_a \cdot (\{\mu_b - \mu_a\} \cdot \mathbf{H}_b) - i\omega \mathbf{E}_a \cdot (\{\varepsilon_b - \varepsilon_a\} \cdot \mathbf{E}_b) - \mathbf{E}_a \cdot (\{\bar{\bar{\sigma}}_b - \sigma_a I_{3\times 3}\} \cdot \mathbf{E}_b)] dV \quad (1)$$

In this expression, I is the current in the coil, S and V are the surface and volume of the anomalous region, respectively, $\mathbf{E}$ and $\mathbf{H}$ are the electric and magnetic fields, respectively, n is the unit normal pointed outward from the boundary of the anomalous region, ω is the angular frequency of the harmonic excitation of the coil, μ is the magnetic permeability of the material, ε is the electric permittivity of the materials, and $I_{3\times 3}$ is the identity tensor. The subscripts a and b refer to conditions when the anomalous region has conductivity equal to the conductivity of the isotropic host, σ_a, and when the region has an anomalous anisotropic conductivity, $\bar{\bar{\sigma}}_b$. It should be noted that although conductivity is the only material property explicitly written as a tensor in this expression, permeability and permittivity could also be tensors here. Under the usual assumption that displacement currents are negligible, the second term in the integrand is negligible. Furthermore, when the material is non-magnetic, as is the case for most titanium alloys, the first term in the integrand also vanishes.

An additional assumption is made in the Born approximation to reduce (1) even further. If the conductivity change from the reference condition to the anomalous condition is low enough, the transmitted fields inside the scatterer can be approximated as being equal to the fields from the reference condition. This effectively turns each b subscript on a field quantity in (1) into an a, yielding the final simplified expression for impedance change as:

$$\Delta Z = \frac{1}{I^2}\int_V \mathbf{E}_a \cdot (\sigma_a I_{3\times 3} - \bar{\bar{\sigma}}_b) \cdot \mathbf{E}_a dV \quad (2)$$

In the case of an isotropic reference state with an axially symmetric coil, the reference fields are known analytically or can be calculated very quickly with a 2D numerical simulation. The spatially dependent anomalous conductivity is known from applying the rotation matrices at each location to the single crystal conductivity tensor. These rotation matrices are either measured using EBSD or they are generated digitally using a synthetic

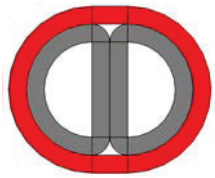

Figure 1. Image of the reflection differential coil configuration. The outside (red) coil is the excitation coil and the inside, d-shaped differential coils (grey) are the receive coils. The receive coils are counter-wound and wired in series.

sample builder. Thus, each term in the integrand is known and the problem has reduced to a numerical integral over the volume of the scatterer. In this case, the volume of the scatterer is the sample microstructure in the vicinity of the coil.

Model Modifications for Reflection Differential Probes

The model described in [5] was never applied to determining the response from a reflection differential probe. A schematic of a reflection differential coil is shown in Fig 1. In this case, equation (1) does not change, but the meaning of the a and b subscripts changes. For the reflection differential coil, the a subscript will refer to the fields established by exciting the inner two coils, counter-wound and connected in series, in the reference isotropic configuration. This can be accomplished by solving for the field from each coil and then superimposing them. The b field is computed by calculating the field established by exciting the outside coil with the microstructure present. However, as in the case of the absolute coil, the Born approximation is made to reduce this computation to simply solving for both a and b fields in the isotropic reference state. Assuming the material is non-magnetic and that the displacement currents are negligible, the new equation for the change in impedance for the reflection differential coil is:

$$\Delta Z = \frac{1}{I^2}\int_V \mathbf{E}_a \cdot (\{\sigma_a I_{3\times 3} - \bar{\bar{\sigma}}_b\} \cdot \mathbf{E}_b) dV \tag{3}$$

Once again, the fields and "anomalous" conductivity are all known at a grid of spatial locations in the vicinity of the coil. Thus, this computation reduces to a numerical integral. However, due to the D-shaped anisotropy of the inner coils, the fields at the surface are now dependent on both radius from the center of the coil as well as the azimuthal direction. This implies that a 2D-axisymmetric simulation for the reference fields is no longer valid, and a full 3D simulation is needed. Furthermore, the computations for the absolute coil at each grid point were accomplished by interpolating the reference field calculated with high fidelity once using a 2D axisymmetric simulation (i.e. a 1-dimensional interpolation). In the case of two split-D coils, or any configuration where the coil deviates from axisymmetric conditions substantially, a 2D interpolation is required to calculate the reference fields at the grid points. This greatly increases simulation times above the typical times required for the absolute coil. The problem is extremely parallelizable, but this has not been implemented in the current iteration of the code.

INITIAL REFLECTION DIFFERENTIAL MODEL VALIDATION

The model was run using EBSD data from a β-annealed Ti-6Al-4V sample with large (1-10 mm diameter) single grains. This sample was used for qualitative validation of the absolute model as well [7]. The EBSD data from the sample is shown in Fig 2. The experiment was performed with a split-D reflection differential probe with a nominal split-D outer diameter of 500 μm. The data set was collected using a Uniwest US-454a eddy current scope. The data was not calibrated to a known calibration notch, so the response of the model was normalized with respect to the

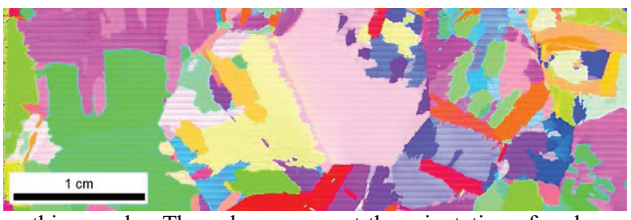

Figure 2. EBSD data collected over this sample. The colors represent the orientation of each crystal with respect to the normal direction of the surface, mapped using an inverse pole figure (IPF). This image was originally shown in [7].

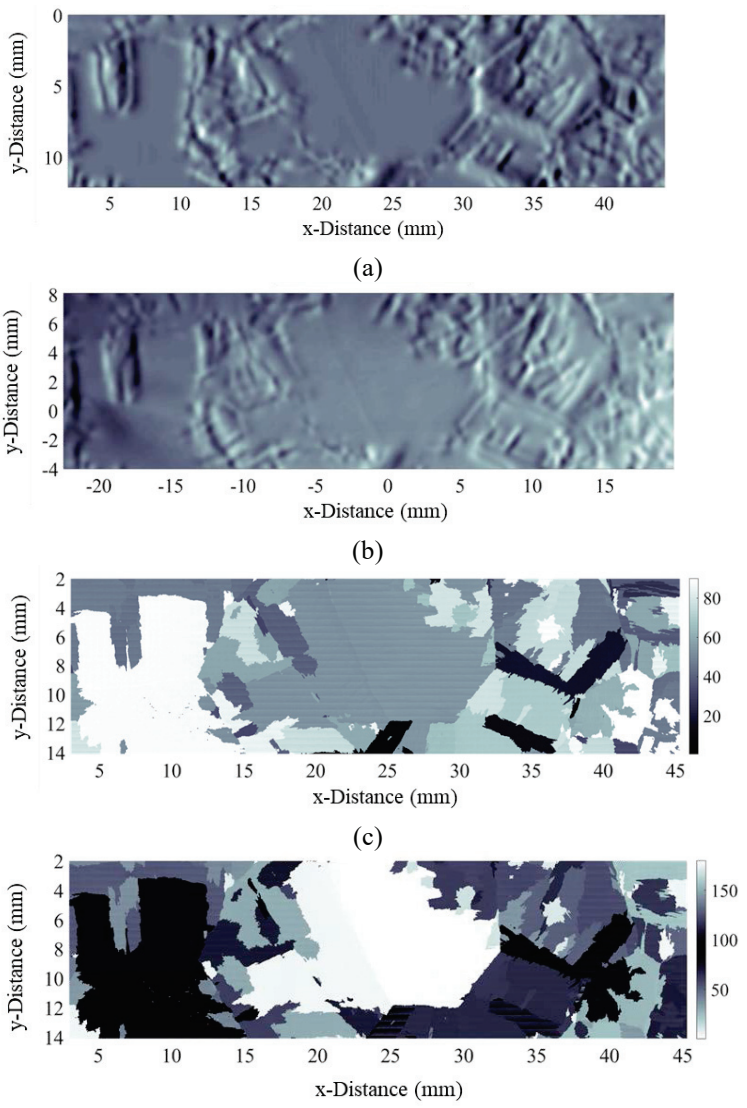

Figure 3. (a) A simulated map of the probe response at each spatial location. (b) An experimental scan collected with the split-D reflection differential coil. (c) A map of the angle of the c-axis if each crystal relative to the normal of the surface.

experimental data. This was accomplished by rotating the phase of the experiment and the model until the signal in the vertical channel was maximized. The vertical signal was then normalized to be within the range [0,1] for both the experiment and the model. The vertical response is shown in the results in this paper. Due to this, only qualitative comparison is made in this paper.

The data from the model and experiment are shown in Fig 3(a) and 3(b) respectively. These two images show relatively good qualitative agreement, especially on the right hand side of the images. A difference map would serve to illuminate this as well as the poor agreement on the left side of the image, but would require careful image registration. At his point, only a qualitative comparison between the two has been done. A spatial map of the tilt of the unique axis (c-axis) of the hexagonal close packed unit cell with respect to the surface is shown in Fig 3(c), and the angle of the c-axis relative to the x-axis of the figure (from here on referred to as the heading of the c-axis) is shown in Fig. 3(d). The color axis of Fig. 4(d) is cyclical to acknowledge the fact that 0 degrees represents the same orientation as 180 degrees. The conductivity of the single crystal is isotropic in the Basal plane of the hexagonal unit cell, thus the primary source of signal for a reflection differential coil will be the tilt of this c-axis. However, for differential coils, the heading of the c-axis could also have a strong signal due to the conductivity changing dramatically in the direction of the differential coils. Any region where there is no change in either of these quantities

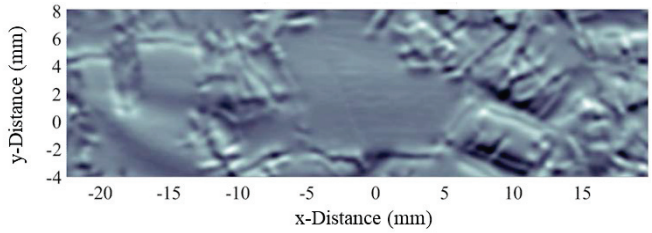

Figure 4. Image of experimental data taken with the probe rotated 90 degrees relative to data shown in Fig 3(b)

should have very little signal. This is best illustrated by viewing the large grain in the middle of the sample. Upon reviewing the EBSD data from Fig. 2, it can be seen that the grain is distinctly split into two regions. This cannot be seen very well in the eddy current image due to the fact that this boundary between the two is a low angle boundary, as can be seen in Fig. 3(c) and Fig. 3(d).

The fact that both of these angles are important for determining the response of the differential coil can be seen by looking at the experimental data shown in Fig. 4. This data was collected with the probe rotated 90 degrees about the out of page axis from the previous coil orientation shown in Fig. 1. Theoretically, this should illuminate the horizontal boundaries between grains better, which can be seen by looking at the upper boundary of the large grain on the left relative to the original experimental data shown in Fig. 3(b). Furthermore, in viewing the lower boundary of the large central grain, the probe sensed this boundary quite well despite the low c-axis tilt change from one region to another, as is shown in Fig. 3(c). This strong signal is explained by the fact that there is sharp contrast between the two regions in c-axis heading, which can clearly be seen in Fig. 3(d). Thus, both orientations of the coil as well as both of the angles describing the direction of the c-axis are crucial for interpretation of the microstructure from an eddy current scan.

TITAINUM MATERIAL WITH MTR

The same probe used for the validation results in the previous section was used to collect data from a sample that had a significant amount of MTRs. This sample was made from Ti811 and had an average MTR diameter of ~250μm. These samples were made as part of another effort related to determining MTR diameter using backscatter ultrasound [1]. The eddy current data collected from these materials is shown in Fig. 5, and is representative of the eddy current signal from titanium alloys used in aerospace applications. With the current probe, even features that have an average diameter of 250μm are not possible to resolve from the eddy current data. This is due to the fact that the spatial resolution of the probe is related to both the physical size of the probe as well as the lateral skin depth [4]. Further signal processing could serve to illuminate larger features, but as noted in the previous section, this would highly depend on the contrast between the orientation of the MTR and the surrounding material as well as the coil orientation.

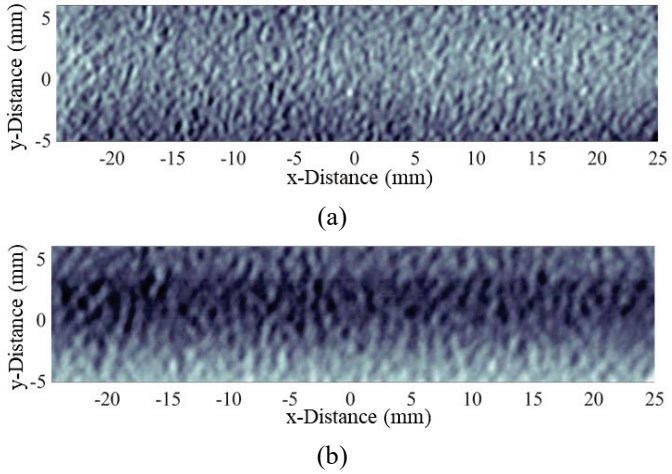

Figure 5. Image of the (a) vertical component and the (b) horizontal component of the eddy current signal collected from Ti811 material with MTRs.

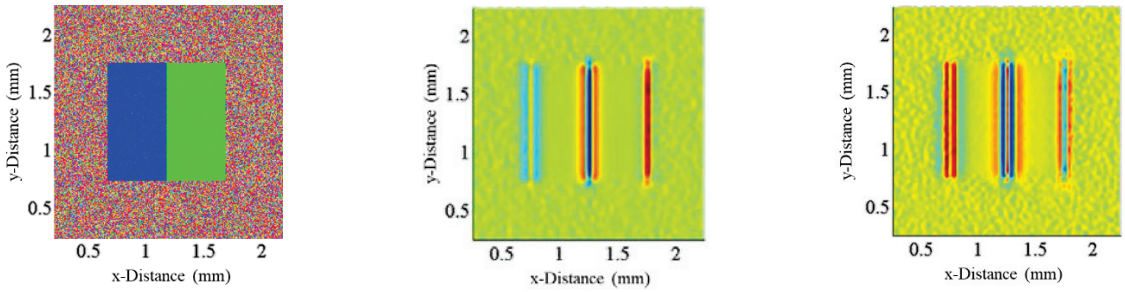

(a) (b) (c)

Figure 6. Image of the (a) inverse pole figure map of the synthetically generated sample with two highly textured regions setting adjacent to one another and surrounded by randomly sampled orientations. The horizontal channel (b) and the vertical channel (c) of the computational eddy current response from this sample are shown as well.

There is an interesting phenomenon that can be noticed in this image related to the spatial correlation length in each of the channels. It can be seen from this data that the number of peaks in the horizontal channel is roughly half the number of peaks seen in the vertical channel. The model was used to determine if this behavior was predicted by the theory. A synthetic sample was generated that had a highly idealized structure shown in Fig. 6(a). Two large regions with strong texture were generated adjacent to one another and surrounded by material with a uniformly sampled distribution of orientations. The horizontal and vertical signals predicted from the model are shown in Fig. 6(b) and Fig. 6(c) respectively. It can be seen from these images that in the particular case of the misorientation shown in Fig. 6(a), the horizontal channel has 3 peaks associated with the boundary between the textured regions and the vertical channel has 5 peaks. Clearly if the phase were changed by 90 degrees, this behavior would switch between the vertical and horizontal channels. This phenomenon could potentially be used to differentiate between the signal from microstructure and the signal from cracks, but more work is needed to fully understand the nature of this signal.

SUMMARY

In this work, a model for predicting the response of a reflection differential coil in the presence of heterogeneous material properties was developed. The model was qualitatively validated against experimental data collected on a large grain Ti-6Al-4V sample. It was observed that differential coils are nearly equally as sensitive to changes in the c-axis tilt and heading orientation. Furthermore, it was shown that the coil is sensitive to the direction of the grain boundaries, implying that the probe can be rotated to give more information about the geometry of the underlying microstructure. The reflection differential coil was used to collect data in a sample with small MTRs, and the data showed a phase-dependent behavior that has not been observed in raw, unprocessed data collected from cracks or notches. This behavior was also observed in the computational model.

ACKNOWLEDGMENTS

L. Homa would like to acknowledge support from the Air Force Research Laboratory through contract number FA8650-14-D-5224.

REFERENCES

1. A. L. Pilchak, J. Li, and S. I. Rokhlin, “Quantitative comparison of microtexture in near-alpha titanium measured by ultrasonic scattering and electron backscatter diffraction”, *Metallurgical and Materials Transactions A* **45A**, 4679-4697 (2014).
2. G. A. D. Briggs and O. V. Kolosov, *Acoustic Microscopy* (Oxford University Press, Oxford, 2010).
3. S. D. Sharples, M. Clark, and M. G. Somekh, “Spatially resolved acoustic spectroscopy for fast noncontact imaging of material microstructure”, *Optics Express* **14(22)**, 10435-10440 (2006).
4. M. Blodgett, W. Hassan, and P. B. Nagy, “Theoretical and experimental investigations of the lateral resolution of eddy current imaging”, *Mat. Eval.* **58(5)**, 647-654 (2000).
5. M. R. Cherry, S. Sathish, R. D. Mooers, A. L. Pilchak, and R. Grandhi, “Moeling of the change of impedance of an eddy current probe due to small changes in host conductivity”, *IEEE Trans. Mag.* **53(5)**, 6201210 (2017).

6. B. A. Auld and J. C. Moulder, "Review of advances in quantitative eddy current nondestructive evaluation", *J. Nondest. Eval*. **18(1)**, 3-36 (1999).
7. M. R. Cherry, S. Sathish, A. L. Pilchak, A. J. Cherry, and M. P. Blodgett, "Characterization of microstructure with low frequency electromagnetic techniques", in *40th Annual Review of Progress in Quantitative Nondestructive Evaluation Volume 33A*, AIP Conference Proceedings 1581, edited by E. E. Chimenti *et al*. (American Institute of Physics, Melville, NY, 2014), pp. 1456-1462.